


## RESEARCH ARTICLE

# Zinc phosphate glass microspheres promoted mineralization and expression of BMP2 in MC3T3-E1 cells

Tianyi Tang<sup>1</sup>  | Ping Kang<sup>2</sup> | Fiona Verisqa<sup>1</sup> | Linh Nguyen<sup>1</sup>  | Jonathan C. Knowles<sup>1</sup> 

<sup>1</sup>Division of Biomaterials and Tissue Engineering, UCL Eastman Dental Institute, Royal Free Hospital, London, UK

<sup>2</sup>Department of Inflammation, Division of Medicine, University College London, London, UK

## Correspondence

Jonathan C. Knowles, Division of Biomaterials and Tissue Engineering, UCL Eastman Dental Institute, Royal Free Hospital, London, UK.  
Email: [j.knowles@ucl.ac.uk](mailto:j.knowles@ucl.ac.uk)

## Abstract

Degradable phosphate glasses have shown favorable properties for tissue engineering. By changing the composition of the glasses, the degradation rate, and ion release are controllable. Zinc oxide can function as a glass network modifier and has been shown to play a positive role in bone formation. Also, phosphate glasses can easily be processed into microspheres, which can be used as microcarriers. This study aims to develop zinc phosphate glasses microspheres and explore the optimized size and composition for applications in bone tissue engineering. Zinc-titanium-calcium-sodium phosphate glasses with 0, 1, 3, 5, or 10 mol % zinc oxide were prepared and processed into microspheres. The smaller microspheres ranged in size from 50 to 106  $\mu\text{m}$ , while the larger ones ranged from 106 to 150  $\mu\text{m}$ . The characteristics of glasses were examined. The osteoblastic cell line MC3T3-E1 was cultured on the surface of microspheres and the cell viability was examined. To evaluate osteogenic differentiation, Alizarin Red S staining, quantitative reverse transcription polymerase chain reaction, and western blot analysis were performed after 14 days. Different sizes of zinc phosphate glass microspheres were successfully made. The glass microspheres with <10 mol % zinc oxide were able to support the adhesion and proliferation of MC3T3-E1 cell lines. The relative gene expression of BMP2 was significantly upregulated in the smaller glass microspheres containing 3 mol % zinc oxide (26-fold,  $p < .001$ ) and both sizes of microspheres containing 5 mol % zinc oxide (smaller: 27-fold,  $p < .001$ ; larger: 35-fold,  $p < .001$ ). Additionally, cluster formation was observed in glass microspheres after 14 days, and the mineralization of MC3T3-E1 cell lines was promoted. Based on these findings, the glass microspheres containing 3–5 mol % of zinc oxide can promote osteogenic differentiation for MC3T3-E1 cells.

## KEYWORDS

bone tissue engineering, osteogenic differentiation, phosphate glasses, zinc oxide

## 1 | INTRODUCTION

Tissue engineering benefits from the successful application of bio-compatible and degradable scaffolds, functional molecules, and cell therapy. Phosphate glass has been studied and shown desirable properties for bone repair. Like other kinds of bioactive glasses, phosphate glass has good biocompatibility and physical properties for bone tissue engineering.<sup>1,2</sup> Moreover, phosphate glass can potentially be used in bone regeneration due to its better degradation properties and active ion release properties.<sup>3</sup> It is precise because of these unique properties that phosphate glass shows potential to be developed as a scaffold for bone tissue regeneration.

The basic network former of phosphate glass is  $P_2O_5$ , but other compounds can be added such as network modifiers.<sup>4,5</sup> In general, these glasses have good wettability but also can lack chemical stability in an aqueous environment and can degrade too quickly and cause large changes in pH values.<sup>6</sup> However, by changing the components, the atomic structure and degradation rate of phosphate glass can be easily modified, and the degradation rate changes over several orders of magnitude. Phosphate glass is also considered a reservoir that stores the active ions essential for bone repair. Calcium and sodium can be glass network modifiers for phosphate glasses as they are also found in abundance in the human skeleton. The weight loss and pH changes of phosphate glass containing CaO and  $Na_2O$  were studied. By increasing the molar percentage of CaO, the durability of phosphate glass can be enhanced. However, according to previous studies, the pH changes of  $CaO-Na_2O-P_2O_5$  glasses can be detrimental to cell growth and limit the application of this phosphate glass compositional range.<sup>7,8</sup>

Therefore, the incorporation of glass network modifiers can be essential depending on the application. It was reported that titanium-doped phosphate glass helped to reduce ion release in a short period and contributed to pH homeostasis. A small amount of  $TiO_2$  was reported to significantly increase the densification of phosphate glasses, but beyond 7 mol %, more  $TiO_2$  did not continue to increase the structural stability further. Further research showed that titanium-calcium-sodium phosphate glass promoted cell proliferation and osteogenic differentiation.<sup>9</sup>

Zinc is an important element in cell growth and differentiation. Previous research successfully developed phosphate glass disks with up to 15 mol % of zinc.<sup>10</sup> It was found that up to 10 mol % of zinc positively affected the osteogenic differentiation of the MG-63 cells. Also, zinc was found to have a role in osteochondral tissue engineering. Eraj et al. found that a lower concentration of ZnO promoted chondrogenic differentiation while a higher concentration stimulated osteogenic differentiation.<sup>11</sup> Infection is a major complication of orthopedic surgery.<sup>12,13</sup> The ion release of zinc was reported to play an anti-bacterial role that may help to reduce the risk of infection after surgery.<sup>6,14</sup>

For wider applications, phosphate glass can be processed into different structural forms, such as glass disks and microspheres.<sup>15,16</sup> With a larger surface area for cell adherence and proliferation, the application of phosphate glass microspheres showed advantages for use as microcarriers.<sup>17,18</sup> Meanwhile, the flame spheroidization

technique is fast and affordable, which benefits the mass production of glass microspheres.<sup>19</sup> The cellular mechanisms of bone remodeling that involve the regulation of osteoclasts and osteoblasts were studied in previous research.<sup>20</sup> Therefore, adapting microcarriers to target cells is crucial. Successful application of microcarriers can not only expand target cells but also be of benefit to cell differentiation.

The size of glass microspheres is another main factor associated with surface area, degradation rate, and ion release.<sup>21</sup> By selecting a certain size range of phosphate glass microspheres, we can explore the optimum growth conditions that promoted proliferation, osteogenic differentiation, or chondrogenic differentiation. This may help us to expand the application of glass microspheres as microcarriers for different seeded cells.

In this study, we developed five different zinc-titanium-calcium-sodium phosphate glasses. For each sample, two different-sized groups of microspheres were prepared. MC3T3-E1 cell lines were cultured, and we explored the potential application of zinc phosphate glass microspheres for bone tissue engineering.

## 2 | MATERIALS AND METHODS

### 2.1 | Materials preparation

#### 2.1.1 | Preparation of zinc phosphate glass

Zinc phosphate glasses were made with melting quenching technology according to the protocols described in the previous research.<sup>19</sup> The details of all samples we used in this study are shown in Table 1. The precursors including phosphorus pentoxide ( $P_2O_5$ ), calcium carbonate ( $CaCO_3$ ), sodium dihydrogen phosphate ( $NaH_2PO_4$ ), titanium dioxide ( $TiO_2$ ), and zinc oxide (ZnO) were more than 98% purity. In brief, precursors were mixed thoroughly and transferred to the crucible. Then, the mixtures were melted at a temperature of 700°C for 30 min and then kept at a temperature of 1300°C for 4 h in the furnace. The final products were poured onto a metal plate and cooled overnight.

#### 2.1.2 | Preparation of microspheres

Two different sizes of glass microspheres were made for each sample. The smaller microspheres were in a size of 50–106  $\mu m$  and the larger

**TABLE 1** Samples and composition.

Glass code	Composition (mol %)				
	ZnO	$P_2O_5$	$Na_2O$	$TiO_2$	CaO
Zn0	0	45	20	3	32
Zn1	1	45	20	3	31
Zn3	3	45	20	3	29
Zn5	5	45	20	3	27
Zn10	10	45	20	3	22

ones were in a size of 106–150  $\mu\text{m}$ . For the manufacturing process, the glasses were ground into particles and sieved by woven wire sieves (200SIW.050, 200SIW.106, 200SIW.150, Endecotts) at first. The flame spheroidization technique was performed to form phosphate glass microspheres.<sup>19</sup> The flame was generated with a blow torch (11901, Monument) fueled by liquefied gas (Vortex Map-X Gas Canister, Arctic Hayes Ltd). This flammable gas contains propylene and propane, which theoretically produce flames exceeding 2900°C in oxygen. The phosphate glass particle flow was regulated using a particle dispenser with a variable control mechanism to ensure a precise and consistent delivery of particles into the flame. Then, samples in each group were collected and sieved to obtain the desired size range of glass microspheres. Images of both smaller and larger glass microspheres were taken, and their sizes were measured using Image-Pro (Premium 9.3, Media Cybernetics).

## 2.2 | Materials characterizations

### 2.2.1 | X-ray diffraction

X-ray diffraction (XRD) was performed to ensure the glass was amorphous. The zinc phosphate glass samples were ground into particles and then processed with the flame spheroidization technique. The XRD analysis was carried out with Bruker D8 Advance Diffractometer. Following the methods described in previous research, we collected data from 10° to 100° and a step size of 0.02° with Ni-filtered Cu K $\alpha$  radiation.<sup>19</sup> The analysis was conducted with OriginPro (2021b, OriginLab).

### 2.2.2 | Fourier transform infrared spectroscopy

Fourier transform infrared spectroscopy (FTIR) was performed to investigate the various structural units that are present in phosphate glasses. The samples were prepared the same as for XRD. FTIR spectra were collected using a Perkin Elmer spectrometer 2000 (Perkin Elmer, Seer Green) with an attenuated total reflectance accessory (Golden Gate, Specac, Orpington). Powder samples were scanned at room temperature in a transmission spectroscopy mode in the range of 600–1800  $\text{cm}^{-1}$  at a 4  $\text{cm}^{-1}$  resolution. Each spectrum was the result of summing eight scans.

### 2.2.3 | Differential thermal analysis

Differential thermal analysis (DTA) studies were conducted with a Setaram differential thermal analyzer. We transferred glass particles to a platinum crucible and recorded the net weights for each sample at first. The carrier gas was nitrogen in this study. Another empty platinum crucible was mounted on the DTA rob as a reference. The samples were heated up to 1000°C with a heating rate of 20°C  $\text{min}^{-1}$ . The glass transition temperature ( $T_g$ ), crystallization temperature ( $T_c$ ),

and melting temperature ( $T_m$ ) were measured and processed with Calisto Processing software (v1.041, Setaram).

### 2.2.4 | Scanning electron microscopy

Scanning electron microscopic (SEM) images were acquired to observe the microspheres, the cells on the surface, and the degradation of the microspheres. For samples without cells, the microspheres were attached to a stub using an adhesive tab. For samples with cells, the samples were prepared following the steps of fixation, dehydration, and sputter coating. The samples were fixed in 3% glutaraldehyde at a temperature of 4°C for 24 h. A series of increasing concentrations of ethanol (50%, 70%, 90%, and 100%) were used for dehydration. Then, the palladium coating was performed by the Polaron E5100 coating device. SEM images (EHT = 9 kV, WD = 6.3 mm) were taken with Zeiss SEM.

### 2.2.5 | Energy-dispersive x-ray spectroscopy

Energy dispersive x-ray spectroscopy (EDS) was performed using a detector (X-act, Oxford Instruments) on an SEM (EVO MA10, Zeiss). The distribution of phosphorus, calcium, sodium, titanium, and zinc on the surface of glass microspheres was mapped at an accelerating voltage of 20.00 kV. Gray-scale images were colorized and merged using ImageJ.

## 2.3 | Cell culture

The osteoblastic cell line MC3T3-E1 (99072810, Sigma-Aldrich) was cultured at a temperature of 37°C and an atmosphere of 5% CO<sub>2</sub> environment. The complete growth medium was prepared in a MEM-based growth medium (11095080, Gibco) with 10% fetal bovine serum (26140079, Gibco) and 1% penicillin–streptomycin (15140122, Gibco), which equals 100 units of penicillin and 100  $\mu\text{g}$  of streptomycin in every 1 mL whole growth medium. Phosphate glass microspheres were sterilized by dry heat at a temperature of 140°C for 3 h and then transferred into cell culture microplates with a low adherent surface (677970, Greiner Bio-One). The microspheres were exposed to UV light for 30 min before the complete growth medium was added. MC3T3-E1 cells were seeded on the surface of phosphate glass microspheres, and the growth medium was changed every 2 days. The cell seeding density was 12,000 per well with phosphate glass microspheres in 48-well plates for downstream experiments, except for the indirect cytotoxicity test in 96-well plates.

## 2.4 | Cell counting kit 8

Cell counting kit 8 (CCK8) was used to evaluate *in vitro* cytotoxicity. To explore the growth conditions for MC3T3-E1 cells, samples with

40 or 60 mg/well microspheres were prepared. The indirect cytotoxicity test experiment was designed based on the standard document ISO 10993-5:2009. For the preparation of extracts, the zinc phosphate glass microspheres were incubated in 400  $\mu$ L complete growth medium for 24 h at 37°C, 5% CO<sub>2</sub>. Then they were diluted using the original extracts into fresh complete growth medium at a concentration of 100%, 75% 50%, and 25%. MC3T3-E1 cells were sub-cultured at monolayers with 5000 per well in 96-well plates overnight and then cultured with 100  $\mu$ L dilution series for another 24 h. The control group was cultured in complete growth medium without extracts. The CCK8 assay was performed following the protocols from a commercial kit (ab228554, Abcam). We aspired growth medium and added 100  $\mu$ L WST-8 working solutions by multichannel pipettes. After incubating for 2 h at 37°C, the samples were measured by an absorbance reader (M200, Tecan) at 460 nm.

For direct contact test, MC3T3-E1 cells were seeded on 40 or 60 mg of zinc phosphate glass microspheres. The cell seeding density was 12,000 per well in 48-well plates with a low adherent surface. These cells were then three-dimensional cultured for 1, 3, and 7 days. At each time point, the CCK8 assay was performed, and data was collected after 2 h of incubation.

## 2.5 | Alizarin Red S staining

The Alizarin Red S assay (ab146374, Abcam) was carried out to detect calcium deposits. MC3T3-E1 cells were cultured in 48-well plates with the cell-repellent surface for 14 days. The growth medium was aspirated and then the samples were washed with PBS buffer (10010015, Gibco) three times. Then the samples were stained with 0.02 g/mL Alizarin Red S solution for 5 min at room temperature. After washing the samples with PBS buffer for another five times, the images were captured with the digital camera with a macro lens and microscope. The glass microspheres without cells were incorporated as the control group with the same process. Then, the Alizarin Red S staining with 800  $\mu$ L of 10% cetylpyridinium chloride (CPC) was destained at 37°C for 24 h. The absorbance of the supernatant was collected with a microplate reader at 560 nm (M200, Tecan).

## 2.6 | Quantitative reverse transcription polymerase chain reaction

Quantitative reverse transcription polymerase chain reaction (RT-qPCR) was performed to detect gene expression in this study. According to the manufacturer's protocols, total RNA was purified using a spin column kit (12183018A, Invitrogen). The cellular samples were treated with lysis buffer containing 40 mM dithiothreitol (DTT). The concentration and purification of total RNA were evaluated by NanoQuant plate on a microplate reader (M200, Tecan). Then, the samples were reverse transcribed (4368814, Applied Biosystems). For long-term stabilization, cDNA was diluted in Tris-EDTA buffer (93302, Sigma-Aldrich) and stored in a -20°C freezer.

**TABLE 2** Gene primers.

Gene	Primer sequence
GAPDH	
Forward	AGGTCGGTGTGAACGGATTG
Reverse	TGTAGACCATGTAGTTGAGGTCA
BMP2	
Forward	GGGACCCGCTGTCTTCTAGT
Reverse	TCAACTCAAATTCGCTGAGGAC
Col10 $\alpha$ 1	
Forward	TTCTGCTGCTAATGTTCTTGACC
Reverse	GGGATGAAGTATTGTGCTCTGGG
Sp7	
Forward	ATGGCGTCCTCTCTGCTTG
Reverse	TGAAAGGTCAGCGTATGGCTT

The gene expressions of osteogenesis-related markers were determined with the SYBR Green PCR reagent kit (A46109, Applied Biosystems) in the Applied Biosystems 7300 Real-Time PCR System. The sequences of primers used in this study are shown in Table 2. Normalized for GAPDH, results were analyzed with DataAssist (Version 3.01, Applied Biosystems).

## 2.7 | Immunofluorescence staining

After aspirating the growth medium and washing it with PBS buffer three times, the samples were fixed with 4% paraformaldehyde (PFA) solution for 15 min at room temperature. A 0.1% Triton-X100 in PBS buffer was prepared for permeabilization and incubated with samples for 15 min at room temperature. To reduce the unspecific binding of the antibody, 2% goat serum in PBS buffer was diluted as well. After blocking for 45 min at room temperature, the samples were incubated with rabbit recombinant monoclonal antibody to BMP2 (1:100, ab214821, Abcam) at 4°C overnight. The Alexa Fluor 488-conjugated secondary antibody (goat anti-rabbit IgG, 1:1000, ab150077, Abcam) and phalloidin-iFluor 647 (1:1000, ab176759, Abcam) were incubated at 37°C for 45 min. Then samples were stained with DAPI for 10 min at room temperature. The samples were washed with PBS buffer (pH 7.4) three times between each step. The images were taken with a confocal fluorescence microscope (Aurox).

## 2.8 | Western blot

MC3T3-E1 cells cultured with zinc phosphate glass microspheres for 14 days were lysed in radioimmunoprecipitation assay (RIPA) buffer supplemented with protease and phosphatase inhibitors. Protein concentrations were determined via BCA assay (23225, Thermo Scientific). Samples were diluted to equal concentrations, boiled, and loaded onto the 4%–20% Criterion™ TGX Stain-Free™ Protein Gels to



run at 250 V for 25 min. Proteins in the gel were then transferred using Trans-Blot Turbo Midi 0.2  $\mu$ m PVDF Transfer Packs and Trans-Blot Turbo Transfer System, according to the manufacturer's protocols. The membranes were then blocked in 5% bovine serum albumin in 1 $\times$  phosphate-buffered saline with Tween (TBST). Membranes were probed with anti-BMP2 (rabbit recombinant monoclonal antibody, 1:2000, ab214821, Abcam) and anti-GAPDH (mouse monoclonal antibody, 1:10,000, 60004-1-Ig, Proteintech) antibodies. After being washed three times with  $\times$ 1 PBST for 10 min each, the HRP-conjugated secondary antibodies (goat anti-rabbit IgG, 1:1000, 7074S, cell signaling; horse anti-mouse IgG, 1:1000, 7076S, cell signaling) were incubated for 1 h at room temperature, and the membranes were subsequently rinsed again. Amersham enhanced chemiluminescence reagents (GE Healthcare) were used to expose the membranes. Semi-quantitative analysis was performed using ImageJ (1.53t, NIH).

## 2.9 | Statistical analysis

The data were expressed as the mean  $\pm$  standard deviation and analyzed by GraphPad Prism 9.3.1. The Shapiro–Wilks test was performed to detect the normality of data distribution and the

homogeneity of variance was tested by Bartlett's test. For the data that did not follow a normal distribution, a non-parametric test was performed. If the data followed a Gaussian distribution and the homogeneity of variance was consistent, the inter-group statistical difference was evaluated by one-way analysis of variance (ANOVA), and Tukey's multiple comparisons were performed as follow-up tests. If the data followed Gaussian distribution but the homogeneity of variance was inconsistent, Welch's ANOVA test and Dunnett's T3 multiple comparisons would be performed.

## 3 | RESULTS

### 3.1 | The zinc phosphate glass microspheres could support the adhesion of MC3T3-E1 cells

Five different zinc phosphate glasses were made and ground into particles. The characteristics of these samples were studied with XRD, FTIR, and DTA. In brief, all these zinc phosphate glasses exhibited a typical XRD pattern of amorphous solids (Figure 1A). Peaks in the FTIR spectra were found around 1256, 1085, and 882  $\text{cm}^{-1}$ , indicating  $\text{PO}_4^{2-}$ ,  $\text{PO}_3^{2-}$ , and P–O–P band, respectively (Figure 1B). The

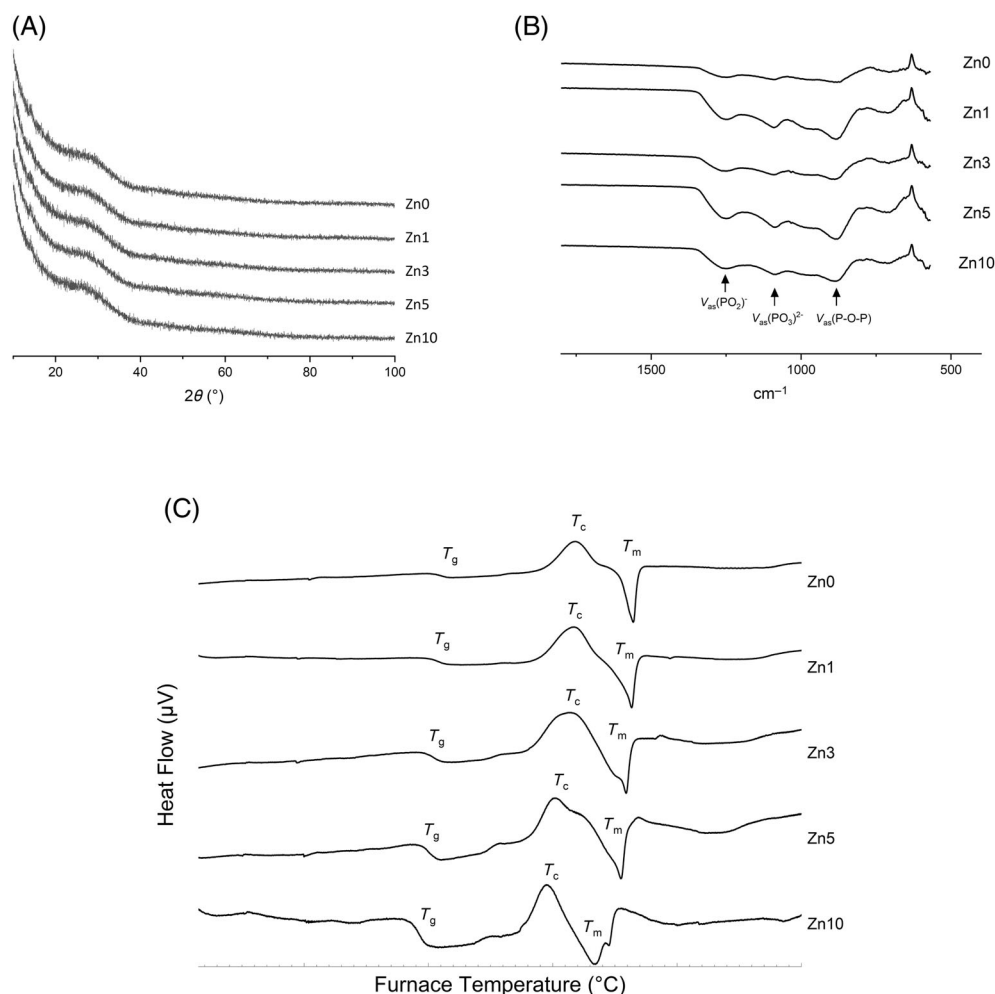


**FIGURE 1** (A) The x-ray diffraction (XRD) patterns of phosphate glasses with 0, 1, 3, 5, or 10 mol % of zinc oxide. The data were collected from  $10^\circ$  to  $100^\circ$  and a step size of  $0.02^\circ$  with Ni-filtered Cu K $\alpha$  radiation. (B) The Fourier transform infrared spectroscopy spectra (FTIR) of zinc phosphate glasses. Glass particles were scanned in a transmittance mode in the range of 600–1800  $\text{cm}^{-1}$  at a 4  $\text{cm}^{-1}$  resolution. The peak of FTIR spectra was detected at wavenumber around 1256, 1085, and 882  $\text{cm}^{-1}$ . (C) Differential thermal analysis (DTA) of zinc phosphate glasses. The samples were heated from 20 to 1000°C with a heating rate of 20°C  $\text{min}^{-1}$ . The glass transition temperature ( $T_g$ ), crystallization temperature ( $T_c$ ), and melting temperature ( $T_m$ ) were determined as a function of zinc oxide content.

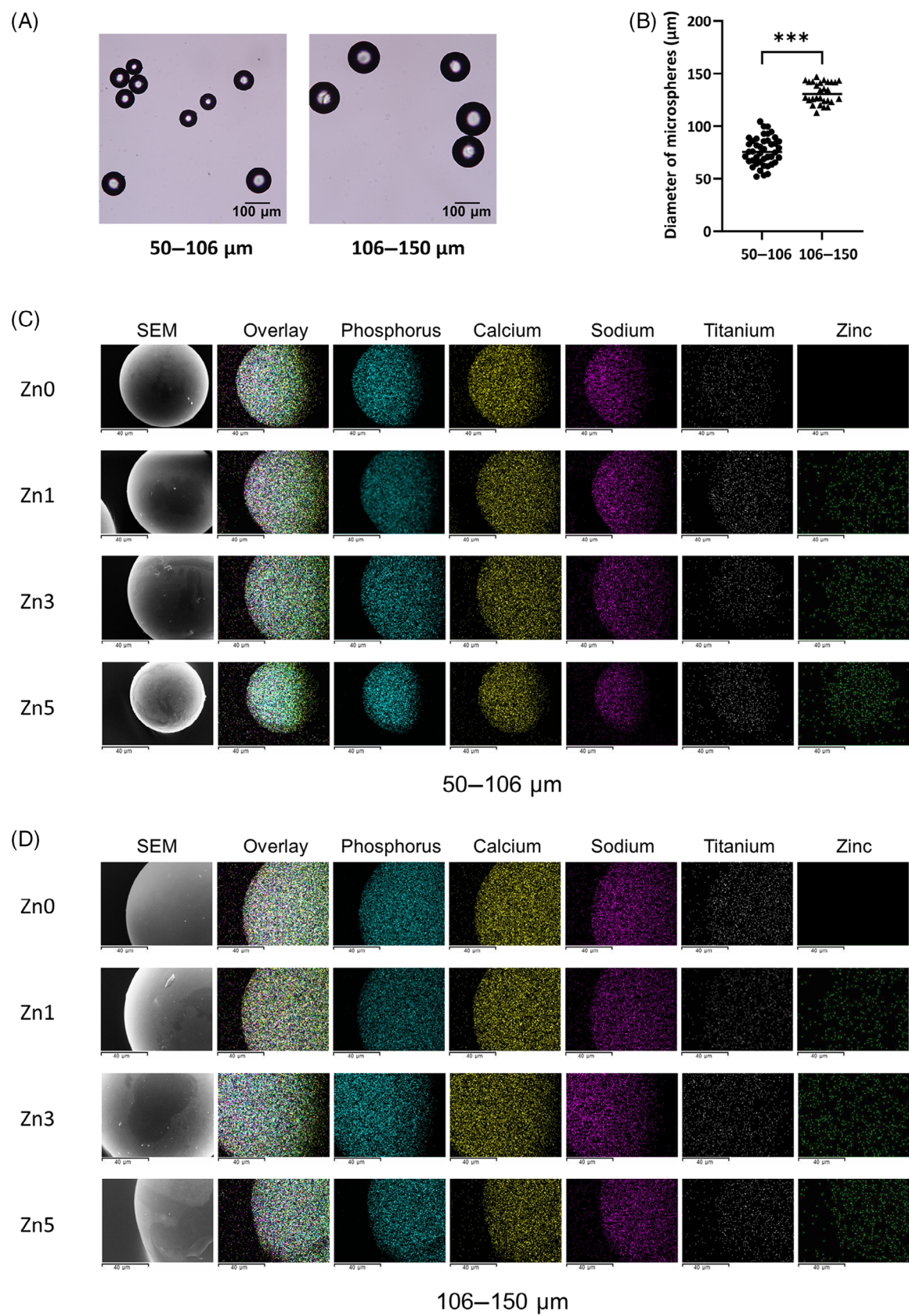
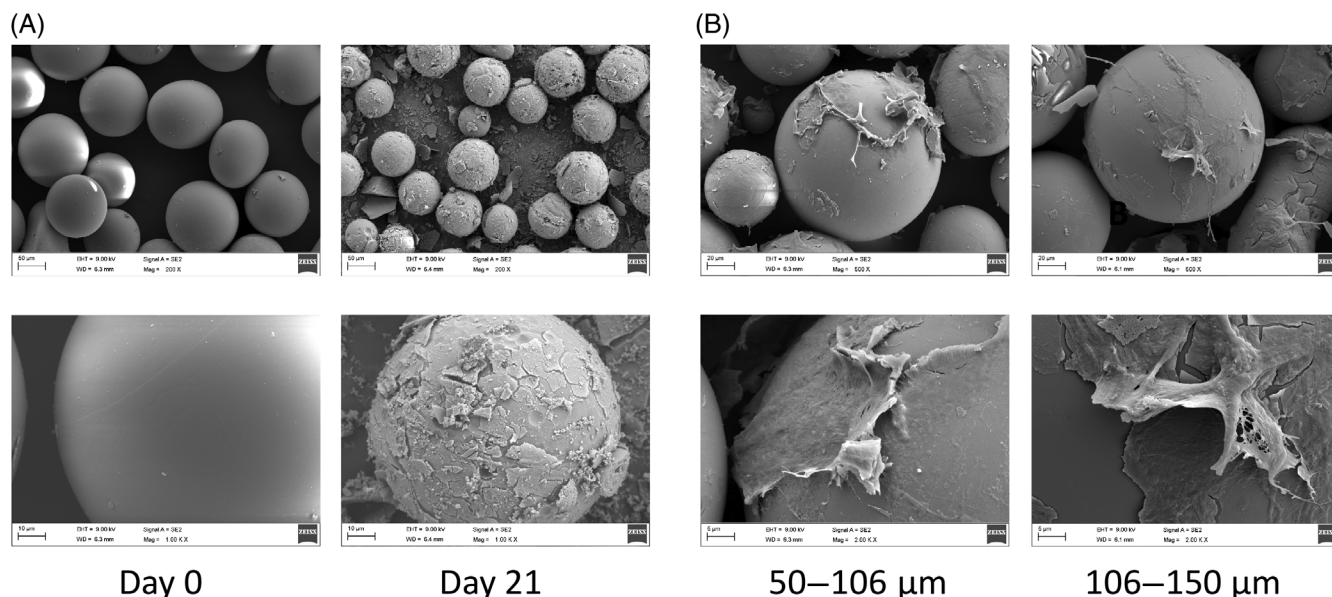


FIGURE 2 Legend on next page.



**FIGURE 3** (A) SEM images of ZnO phosphate glass microspheres incubated with cell growth medium at 37°C, 5% CO<sub>2</sub> for 0 and 21 days. (B) SEM images of MC3T3-E1 cell line cultured on the surface of ZnO glass microspheres overnight.

difference in the content of calcium oxide and zinc oxide changed the  $T_g$ ,  $T_m$ , and  $T_c$  temperatures. We found that an increase of zinc oxide in phosphate glasses decreased glass transition temperature (Figure 1C).

The zinc phosphate glass microspheres were prepared successfully with flame spheroidization technology. We applied a modified production process to collect microspheres in two different size groups (Figure 2A). The size distributions of microspheres from both the smaller and the larger size groups were measured and could be used in the following study (Figure 2B). Homogeneous distribution of phosphorus, calcium, sodium, titanium, and zinc was seen on the surface of glass microspheres in both size groups (Figure 2C,D).

SEM images show that these zinc phosphate glass microspheres are degradable in cell growth medium (Figure 3A). To avoid undesired adherence when doing cell culture, microplates with cell-repellent surfaces were used. MC3T3-E1 cells were seeded on the glass microspheres and incubated at 37°C, 5% CO<sub>2</sub> overnight. Both size groups of microspheres supported the adherent of cells (Figure 3B). The following experiment investigated the growth and migration of MC3T3-E1 cells with glass microspheres after 7 days. Cells are distributed on the surface of these glass microspheres. The images taken by confocal microscope are shown in Data S1.

### 3.2 | The zinc phosphate glass microspheres exhibited cytocompatibility with MC3T3-E1 cells

To determine the appropriate amount of zinc phosphate glass microspheres for cell culture, MC3T3-E1 cells were cultured with 40 or 60 mg of glass microspheres in 48-well plates with a low adherent surface. After 1 week of cell culture, cluster formation was observed with 40 mg of glass microspheres. For 60 mg glass microspheres, cluster formation could be observed in both size groups of Zn0, Zn1, Zn3, and Zn5 glass microspheres (Figure 4A). However, no such kind of phenomenon was observed in Zn10 glass microspheres.

CCK8 assay was performed to examine cell viability and to explore the effect of different amounts of microspheres in cell culture. The content of zinc oxide could affect cell culture, especially the evidence from 60 mg glass microsphere extracts (Figure 4B). Meanwhile, as the cell viability of MC3T3-E1 cells cultured with extracts from 40 mg of Zn0, Zn1, Zn3, and Zn5 microsphere did not decrease with a lower dilution ratio, the 40 mg of glass microspheres might be better to be used for culturing MC3T3-E1 cells in 48-well plates. Furthermore, MC3T3-E1 cells were seeded directly on the glass microspheres and cultured in three dimensions for up to 7 days. The results showed increasing metabolic activity of MC3T3-E1 cells with 40 mg of zinc phosphate glass microspheres during the observation period.

**FIGURE 2** (A) Microscopy images of zinc phosphate glass microspheres in two different size groups. (B) The diameter of the zinc phosphate glass microspheres in 50–106 μm size group and 106–150 μm size group was measured using Image-Pro (76.27 ± 13.19 and 131.8 ± 10.09 μm, respectively). For each group, we randomly photographed three different microscope fields and marked the sizes of microspheres on the scatter plot. \* $p < .05$ , \*\* $p < .01$ , and \*\*\* $p < .001$ . (C) The scanning electron microscopy (SEM) and Energy-dispersive x-ray spectroscopy (EDS) analysis of glass microspheres in 50–106 μm size group. (D) The SEM and EDS analysis of glass microspheres in 106–150 μm size group. The EDS data collection time was set to collect 2500 counts for each sample.



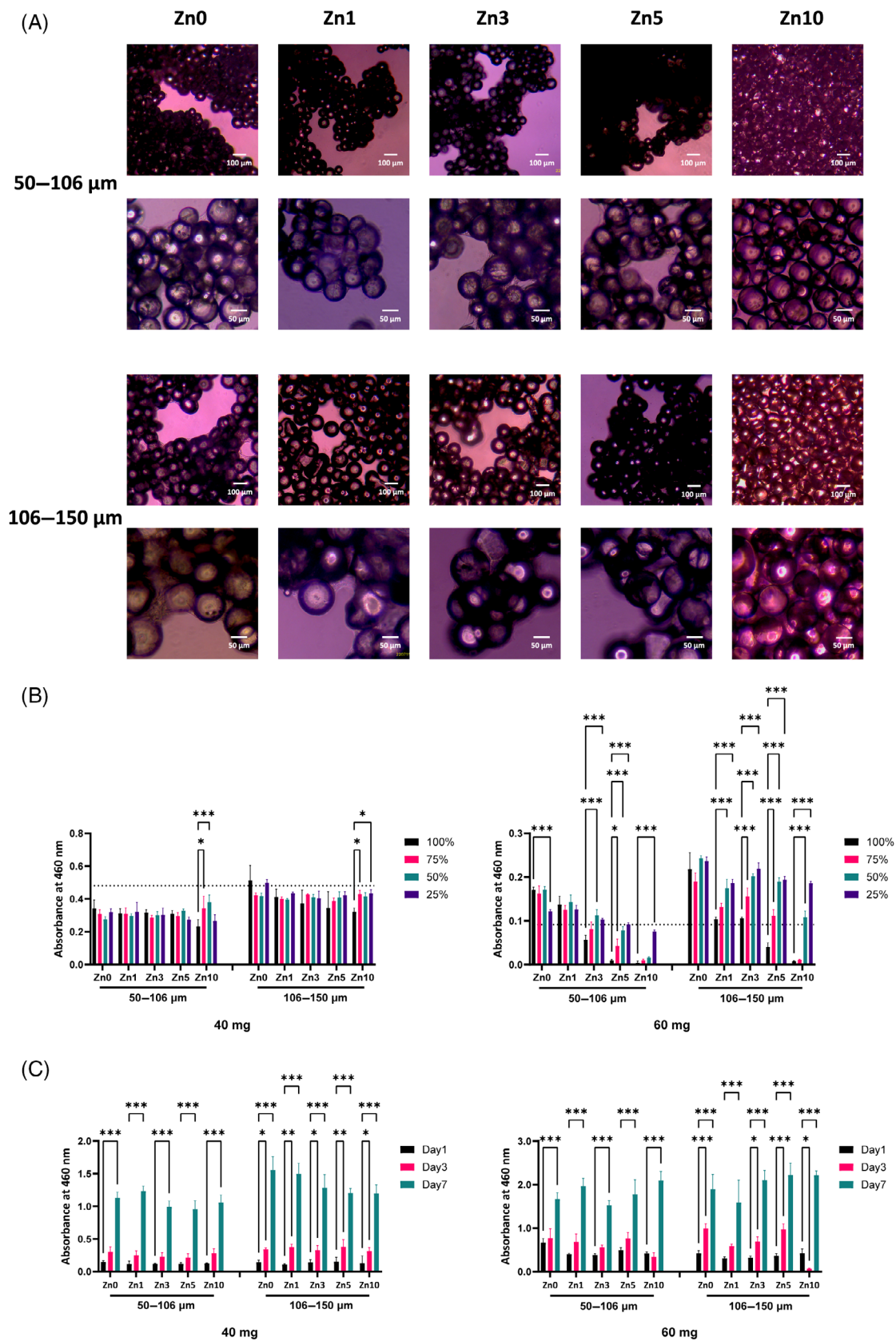


FIGURE 4 Legend on next page.

(Figure 4C). For 60 mg of Zn10 microspheres in the 106–150  $\mu\text{m}$  size group, cell viability was decreased on Day 3 but showed recovery on Day 7. In general, zinc phosphate glass microspheres showed good cytocompatibility with MC3T3-E1 cells in this study. Based on current results, we cultured MC3T3-E1 cells with 40 mg Zn0, Zn1, Zn3, and Zn5 microspheres in the following study.

### 3.3 | The zinc phosphate glass microspheres supported growth and calcification in the MC3T3-E1 cell

As the cluster formation of zinc phosphate glass microspheres was found, the growth of MC3T3-E1 cells with glass microspheres was further explored. The nuclear and cytoskeleton of cells were labeled after 2 weeks (Figures 5 and 6). Stack images captured by confocal microscopy suggested that the cells proliferated on and around glass microspheres. The glass microspheres provided a larger surface area for cell culture compared with a plain surface. Besides, both smaller and larger sizes of zinc phosphate glass microspheres generated three-dimensional cell culture conditions for MC3T3-E1 cells.

To detect the calcium deposits formed during cell culture, Alizarin Red S staining was performed (Figures 7A and S1). The results from 2D cultured MC3T3-E1 cells and positive control were shown in the Data S1. The phosphate glass microspheres without cells were incorporated as the control groups and the quantitative analysis was performed to determine the baseline data (Figure 7C). In general, both size groups of Zn0, Zn1, Zn3, and Zn5 glass microspheres supported the mineralization of MC3T3-E1 cells after 14 days. Furthermore, compared with the phosphate glass microspheres without zinc oxide, the calcification of MC3TC-E1 cells with 3 and 5 mol % of zinc oxide was significantly higher in the 106–150  $\mu\text{m}$  size group (Figure 7B).

### 3.4 | The zinc phosphate glass microspheres promoted the osteogenic differentiation of MC3T3-E1 cells

MC3T3-E1 cells were cultured on the smaller and larger size groups of microspheres for 14 days. The expression of BMP2 in the MC3T3-E1 cell line was found in the smaller and larger size groups. Furthermore, the relative quantification analysis of the genes related to osteogenic differentiation was performed (Figure 8). Compared with the 2D cultured control group, the relative gene expression of

BMP2, Sp7, and Col10 $\alpha$  were upregulated by phosphate glass microspheres. Besides, the higher amount of zinc oxide has a positive impact on osteogenesis differentiation. Zn3 in smaller size and Zn5 significantly increased the gene expression of BMP2. We found that the size difference might be another factor that affected the osteogenesis differentiation. Compared with Zn0, the larger size of Zn5 microspheres promoted the gene expression of Sp7 while the smaller size did not.

To semi-quantitatively analyze the effect of zinc phosphate glass microspheres on osteogenesis differentiation. The total protein from cells cultured with different sizes and content of zinc phosphate glass microspheres was measured. The western blot analysis was conducted afterward. The data showed that the expression of BMP2 was significantly increased by the smaller size of Zn5 glass microspheres (Figure 9).

## 4 | DISCUSSION

In this study, the potential application of zinc phosphate glass microspheres as microcarriers was investigated, focusing on modifying their composition and structural characteristics to apply in bone tissue engineering. Phosphate glass, known for its degradable biomaterial properties, exhibits active ion release, which significantly influences cell behavior.<sup>22,23</sup> The optimization of degradation rate and ion release is crucial, as it can either promote cell growth and differentiation or impede cell survival and disrupt pH homeostasis.<sup>15</sup>

Our previous research found that the titanium oxide in phosphate glass contributes to improved stability, effectively solving issues caused by rapid degradation.<sup>5,24</sup> The ion release and degradation rates of phosphate glass containing up to 15 mol % of titanium oxide were reported.<sup>5,19</sup> Based on these findings, we added 3 mol % of titanium oxide in all the samples. The characteristics of the samples aligned with our previous research, revealing an amorphous structure identified through XRD.<sup>19</sup> Besides, the distribution of zinc and titanium was mapped with EDX and showed similar properties.

A novel and simple approach by employing a series of simultaneous flame spheroidization techniques was introduced in this study.<sup>18</sup> We employed a semi-automated production line when preparing samples, which is beneficial to control systematic bias caused by flame spheroidization. The surface pattern of phosphate glass microspheres was checked with SEM and the size distributions in all groups were measured. In general, we successfully applied the improved method to make glass microspheres in a highly effective

**FIGURE 4** MC3T3-E1 cells were cultured with two size groups of zinc phosphate glass or extracts to examine cytocompatibility. The smaller size group ranges from 50 to 106  $\mu\text{m}$ . The larger size group ranges from 106 to 150  $\mu\text{m}$ . (A) Microscope images of MC3T3-E1 cell line cultured with 60 mg of zinc phosphate glass microspheres for 14 days. (B) CCK8 assay results on extracts. The extracts were prepared by incubating 40 or 60 mg zinc phosphate glass microspheres for 24 h in 400  $\mu\text{L}$  cell growth medium at 37°C, 5% CO<sub>2</sub>. MC3T3-E1 cells were cultured with diluted extracts for 24 h. The cells cultured with complete growth medium are shown in grid lines.  $n = 3$ , \* $p < .05$ , \*\* $p < .01$ , and \*\*\* $p < .001$ . (C) CCK8 assay results by direct contact. MC3T3-E1 cells were cultured on 40 or 60 mg zinc phosphate glass microspheres in 48-well plates with a low adherent surface for 1, 3, and 7 days.  $n = 3$ , \* $p < .05$ , \*\* $p < .01$ , and \*\*\* $p < .001$ .

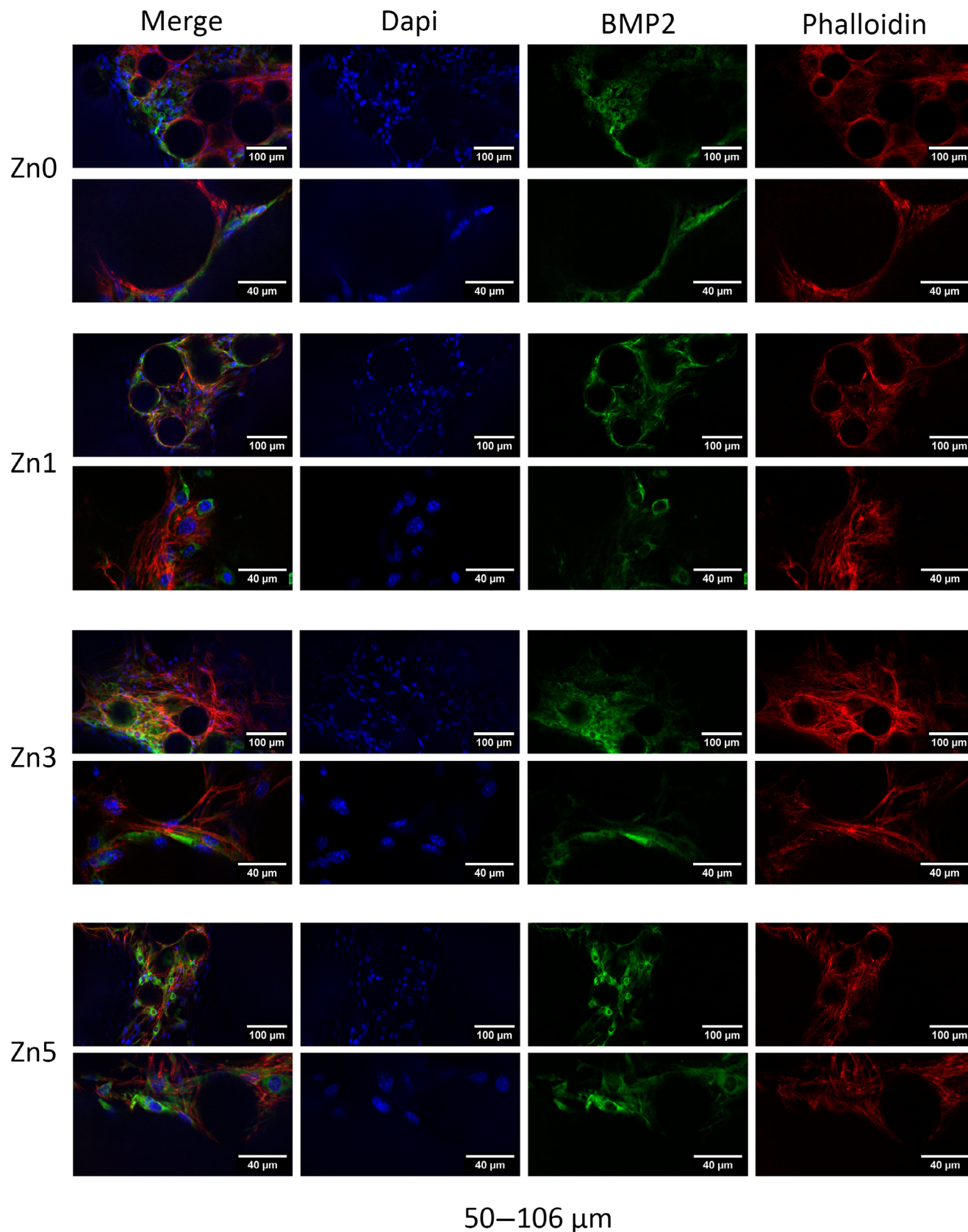


**FIGURE 5** Immunofluorescence staining of DAPI, phalloidin, and BMP2. MC3T3-E1 cells were cultured on 40 mg zinc phosphate glass microspheres. The Zn0, Zn1, Zn3, and Zn5 glass microspheres were in a size of 50–106  $\mu\text{m}$ . The confocal immunofluorescence microscopy images were taken at  $\times 20$  and  $\times 60$ . Scale bars are 100 or 40  $\mu\text{m}$  (bottom row), respectively.



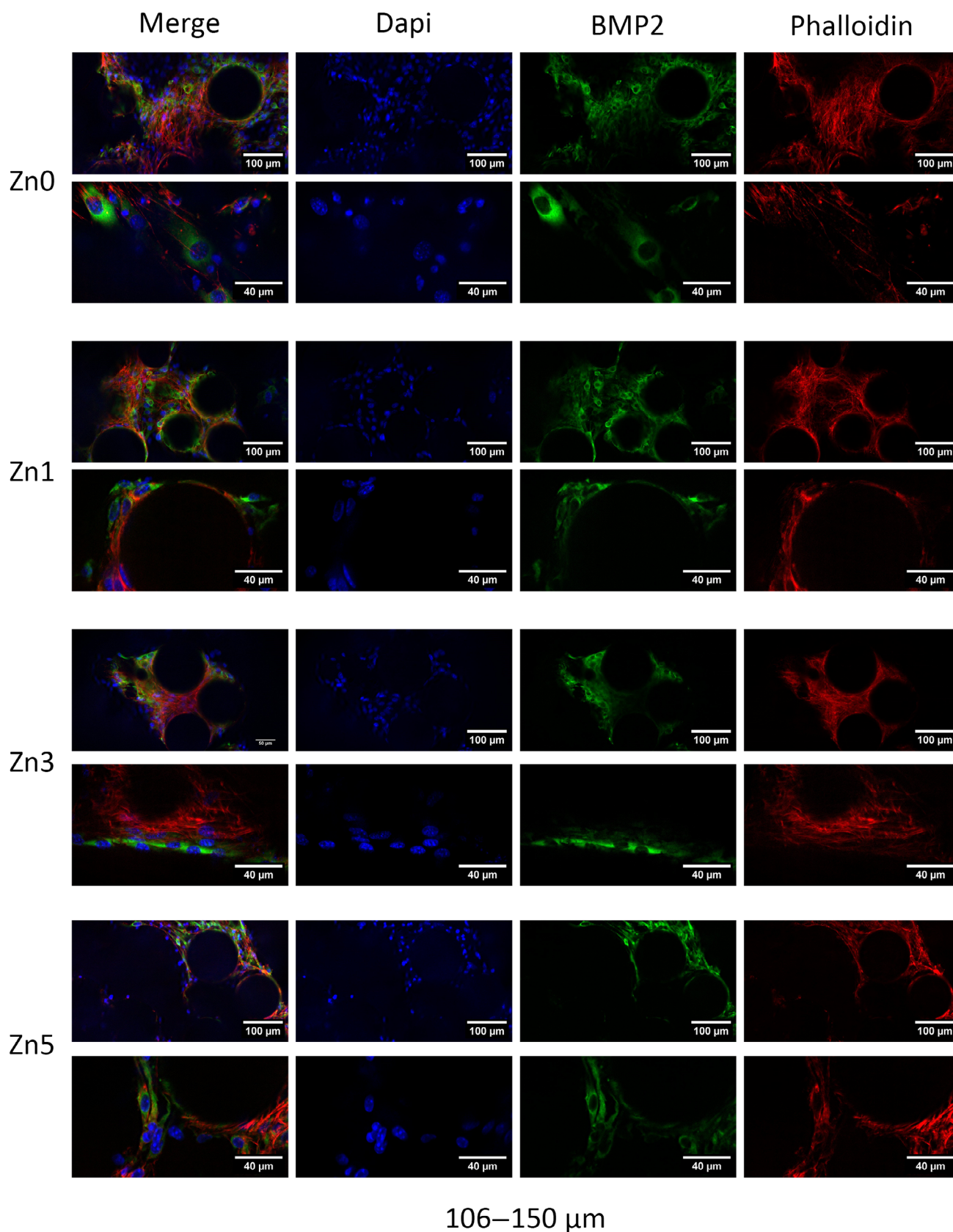


**FIGURE 6** Immunofluorescence staining of DAPI, Phalloidin, and BMP2. MC3T3-E1 cells were cultured on 40 mg zinc phosphate glass microspheres. The Zn0, Zn1, Zn3, and Zn5 glass microspheres were in a size of 106–150 μm. The confocal immunofluorescence microscopy images were taken at  $\times 20$  and  $\times 60$ . Scale bars are 100 or 40 μm, respectively.

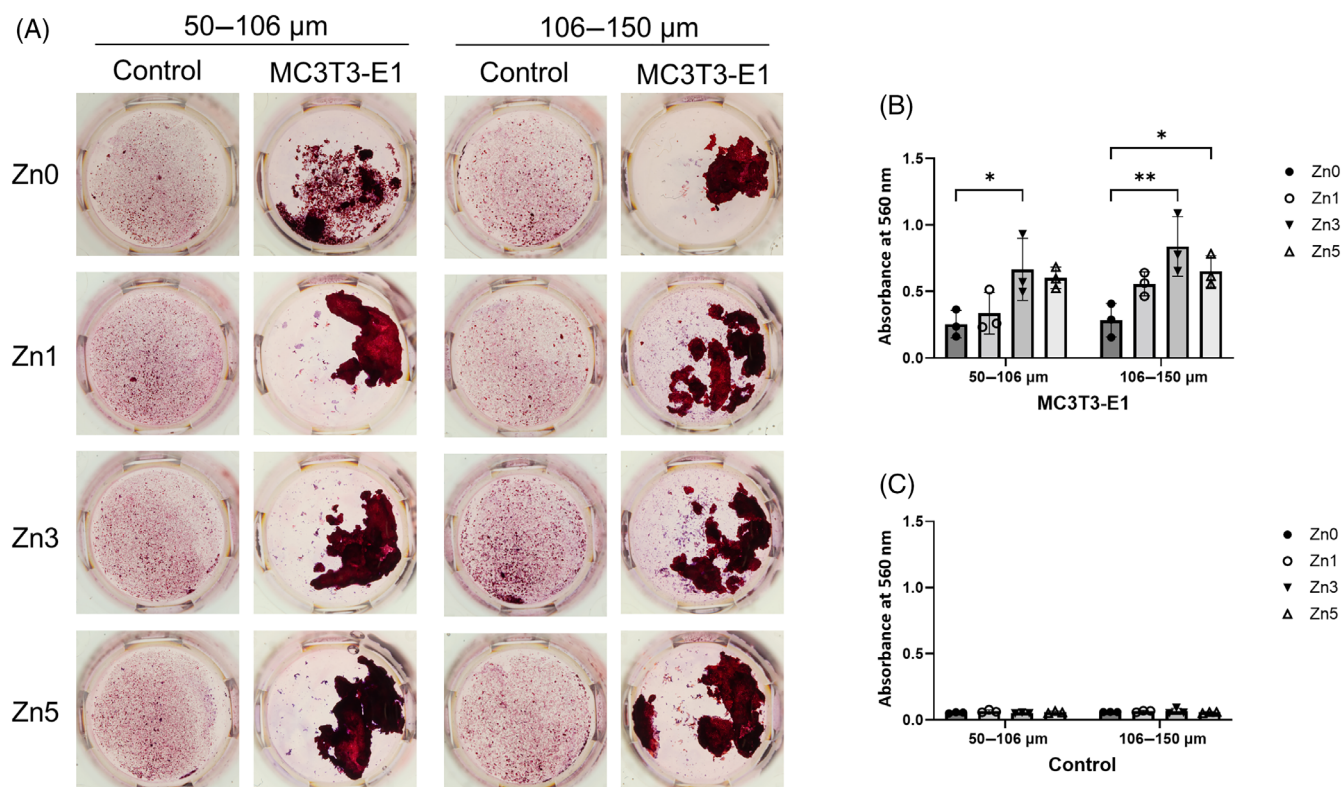


**FIGURE 7** Alizarin Red S staining was performed to detect the in vitro mineralization of MC3T3-E1 cells. (A) Zinc phosphate glass microspheres were transferred to 48-well plates with a cell-repellent surface. The MC3T3-E1 cells were cultured with 40 mg of glass microspheres for 14 days. The control group consisted of the same amount of microspheres without cells. (B,C) The samples, with or without MC3T3-E1 cells, were destained with 800  $\mu$ L of 10% cetylpyridinium chloride for 24 h. The absorbance was read at 560 nm for all samples.  $n = 3$ , \* $p < .05$ , \*\* $p < 0.01$ , and \*\*\* $p < .001$ .

way. MC3T3-E1 cells were able to adhere to the surface of zinc phosphate glass microspheres. The use of phosphate glass microspheres as microcarriers for cell culture is promising not only because of the large surface area for cell growth but also because they facilitate three-dimensional cell culture (Figure S2). The immunofluorescence staining images confirmed these properties, which are consistent with other research and potentially beneficial for differentiation.<sup>25</sup>

Furthermore, the investigation was extended to explore the role of zinc oxide in further enhancing the performance of these microcarriers. The content of zinc oxide was found to affect the cell viability.<sup>10</sup> Previous studies explored the application range of zinc oxide in phosphate glass disks for cell culture and suggested using less than 15 mol % of zinc oxide.<sup>26</sup> Compared with glass disks, the microspheres have a larger surface area, higher degradation rate, and ion release. The MC3T3-E1 cells were cultured with extracts for 24 h and glass microspheres for up to 21 days. The results aim to contribute valuable insights into the application of zinc phosphate glass microspheres as promising microcarriers in tissue engineering and regenerative medicine.

The cell viability was tested with serially diluted extractions from microspheres containing 0 to 10 mol % zinc oxide at first. For 60 mg of zinc phosphate glass microspheres, the higher concentrations of extracts decreased the cell viability compared with lower

concentrations. However, this trend was not obvious for 40 mg glass microspheres. These data suggested that phosphate glass microspheres with zinc could support the growth of the MC3T3-E1 cells, but a high concentration of zinc oxide may affect cytocompatibility, which is consistent with earlier findings on glass disks.<sup>10</sup>

Then, cells were seeded on the surface of glass microspheres directly to confirm this hypothesis. The cell viability was largely affected by the amount of glass microspheres and the content of zinc oxide. A lower concentration of zinc oxide seemed to promote cell growth, but we also found that continuously increasing concentration of zinc oxide in microspheres had a negative impact on the growth of MC3T3-E1 cells. The Zn10 decreased cell viability to MC3T3-E1 cells. Besides, our data suggested that 40 mg of zinc phosphate glass microspheres in 48-well plates is suitable for expanding the cells in vitro. Therefore, the application range of zinc oxide was confirmed and 40 mg microspheres with no more than 5 mol % zinc oxide were used in the following test for osteogenic differentiation.

Previously published work indicated that titanium oxide can not only able to stabilize the glass network structure but also promote differentiation.<sup>9</sup> All our samples contain 3 mol % titanium but with different concentrations of zinc oxide. Compared with Zn0 samples with the control group, our results supported the hypothesis that titanium-doped phosphate glass microspheres can promote

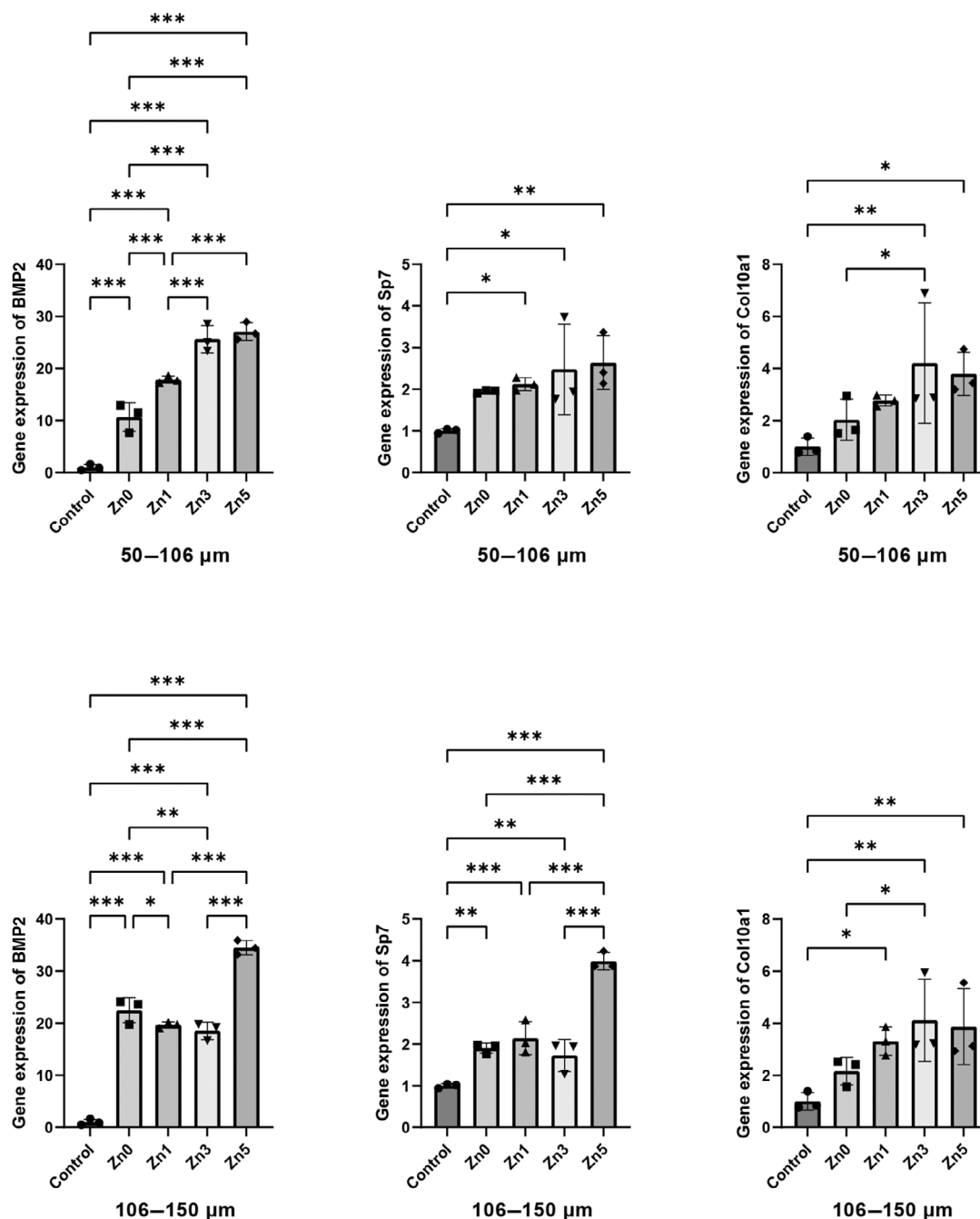


**FIGURE 8** The relative gene expression of BMP2, Sp7, and Col10a1. The total RNA from 2D cultured MC3T3-E1 cells was extracted as the control group. Two different size groups of Zn0, Zn1, Zn3, and Zn5 glass microspheres were prepared as well. MC3T3-E1 cells were cultured on 40 mg zinc phosphate glass microspheres in 48-well plates with a low adherent surface for 14 days.  $n = 3$ ,  $*p < .05$ ,  $**p < .01$ , and  $***p < .001$ .

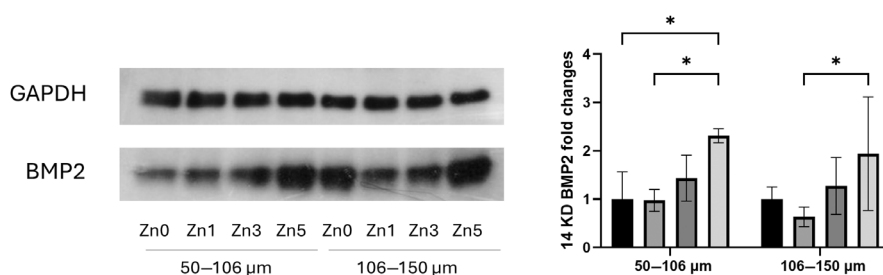


**FIGURE 9** The western blot analysis of anti-BMP2 antibody with MC3T3-E1 cell lines. The fold changes of 14 KD BMP2 were calculated. The expression of BMP2 was significantly promoted by a 50 to 106 μm size group of Zn5 glass microspheres.  $n = 3$ ,  $*p < .05$ .



osteogenic differentiation. We further explored the advantages of zinc oxide in phosphate glass. Compared with ZnO microspheres, Zn3 and Zn5 microspheres exhibited higher expression of osteogenesis-related genes. The western blot analysis supported this finding. The expression of BMP2 is significantly increased with Zn5 glass microsphere after 14 days. The titanium-doped phosphate glass microspheres containing 3–5 mol % of zinc oxide are more conducive to osteogenic differentiation than the control group and glass microspheres without zinc oxide. We acknowledge that the absence of a positive control group, like MC3T3-E1 cells cultured in osteogenic differentiation medium, is a limitation of our study design. Including such a control group would have provided a more comprehensive comparison to assess the osteogenic differentiation induction effect of zinc phosphate glass microspheres.

The size of glass microspheres is another factor that we explored. Microspheres that are smaller than the average diameter of cells are considered hard to support cell adherence.<sup>27</sup> Therefore, glass microspheres larger than 50 µm were collected for culturing MC3T3-E1 cells in this study. The size of smaller microsphere samples ranges from 50 to 106 µm and the larger ones from 106 to 150 µm. This is also the size that is suitable for flame spheroidization as previously described. The smaller or larger size of microspheres also has a different rate of degradation and ion release, which can affect proliferation and differentiation. Both the smaller size group and larger size group of glass microspheres were able to support the adherent of cells. The CCK8 results showed the difference in cell culture between smaller and larger size groups. The surface area for cell adherence and degradation rate might be the factors. For Zn3 glass, the smaller size group of microspheres was taking advantage of osteogenic differentiation compared with the larger size group. Also, the smaller size of Zn5 microspheres significantly promoted the expression of BMP2 than ZnO microspheres. Meanwhile, both size groups of phosphate glass microspheres supported the calcification of MC3T3-E1 cells in this study. Further experiments are needed to explore the factor of size in the degradation and ion release of glass microspheres.

## 5 | CONCLUSION

Zinc phosphate glass microspheres with a zinc oxide content of <10 mol % hold significant promise as microcarriers for bone tissue engineering. These microspheres have shown several advantageous properties that make them suitable for this application. The key finding here is that glass microspheres containing 3–5 mol % of zinc oxide have been shown to promote osteogenesis differentiation for MC3T3-E1 cells. Microcarriers are used to provide structural support for cells during tissue engineering. The size of these microspheres can be customized to meet the specific requirements of target tissues, and their cytocompatible nature ensures that they do not interfere with cellular processes. The stimulation of osteogenic gene expression, protein expression and enhanced mineralization observed in these microspheres make them promising candidates for future research and development in regenerative medicine for bone tissue repair.

## AUTHOR CONTRIBUTIONS

**Tianyi Tang:** Conceptualization; investigation; methodology; validation; visualization; writing—original draft preparation. **Ping Kang:** Methodology; validation; visualization; writing—review and editing. **Fiona Verisqa:** Methodology; writing—review and editing. **Linh Nguyen:** Supervision; writing—review and editing. **Jonathan C. Knowles:** Conceptualization; project administration; supervision; writing—review and editing.

## CONFLICT OF INTEREST STATEMENT

The authors declare no conflicts of interest.

## DATA AVAILABILITY STATEMENT

The data that support the findings of this study are available from the corresponding author upon reasonable request.

## ORCID

Tianyi Tang  <https://orcid.org/0000-0002-6169-9383>

Linh Nguyen  <https://orcid.org/0000-0002-8532-8296>

Jonathan C. Knowles  <https://orcid.org/0000-0003-3917-3446>

## REFERENCES

1. Shirliff VJ, Hench LL. Bioactive materials for tissue engineering, regeneration and repair. *J Mater Sci*. 2003;38(23):4697–4707. doi:[10.1023/a:1027414700111](https://doi.org/10.1023/a:1027414700111)
2. Ryu JH, Mangal U, Lee MJ, et al. Effect of strontium substitution on functional activity of phosphate-based glass. *Biomater Sci*. 2023;11(18):6299–6310. doi:[10.1039/d3bm00610g](https://doi.org/10.1039/d3bm00610g)
3. Abou Neel EA, Pickup DM, Valappil SP, Newport RJ, Knowles JC. Bioactive functional materials: a perspective on phosphate-based glasses. *J Mater Chem*. 2009;19(6):690–701. doi:[10.1039/b810675d](https://doi.org/10.1039/b810675d)
4. Knowles JC. Phosphate based glasses for biomedical applications. *J Mater Chem*. 2003;13(10):2395–2401. doi:[10.1039/b307119g](https://doi.org/10.1039/b307119g)
5. Abou Neel EA, Chrzanowski W, Knowles JC. Effect of increasing titanium dioxide content on bulk and surface properties of phosphate-based glasses. *Acta Biomater*. 2008;4(3):523–534. doi:[10.1016/j.actbio.2007.11.007](https://doi.org/10.1016/j.actbio.2007.11.007)
6. Oh SH, Jung YS, Lee MJ. Assessment of zinc-bound phosphate-based glass-coated denture-relining material with antifungal efficacy for inhibiting denture stomatitis. *Nanomaterials*. 2022;12(17):3048. doi:[10.3390/nano12173048](https://doi.org/10.3390/nano12173048)
7. Uo M, Mizuno M, Kuboki Y, Makishima A, Watari F. Properties and cytotoxicity of water soluble Na<sub>2</sub>O–CaO–P<sub>2</sub>O<sub>5</sub> glasses. *Biomaterials*. 1998;19(24):2277–2284. doi:[10.1016/s0142-9612\(98\)00136-7](https://doi.org/10.1016/s0142-9612(98)00136-7)
8. Ahmed I, Lewis M, Olsen I, Knowles JC. Phosphate glasses for tissue engineering: part 1. Processing and characterisation of a ternary-based P<sub>2</sub>O<sub>5</sub>–CaO–Na<sub>2</sub>O glass system. *Biomaterials*. 2004;25(3):491–499. doi:[10.1016/S0142-9612\(03\)00546-5](https://doi.org/10.1016/S0142-9612(03)00546-5)
9. Lakhkar NJ, Day RM, Kim HW, et al. Titanium phosphate glass microcarriers induce enhanced osteogenic cell proliferation and human mesenchymal stem cell protein expression. *J Tissue Eng*. 2015;6. doi:[10.1177/2041731415617741](https://doi.org/10.1177/2041731415617741)
10. Qaysi MA, Petrie A, Shah R, Knowles JC. Degradation of zinc containing phosphate-based glass as a material for orthopedic tissue engineering. *J Mater Sci Mater Med*. 2016;27(10):157. doi:[10.1007/s10856-016-5770-x](https://doi.org/10.1007/s10856-016-5770-x)
11. Mirza EH, Pan-Pan C, Ibrahim W, Djordjevic I, Pingguan-Murphy B. Chondroprotective effect of zinc oxide nanoparticles in conjunction with hypoxia on bovine cartilage-matrix synthesis. *J Biomed Mater Res A*. 2015;103(11):3554–3563. doi:[10.1002/jbm.a.35495](https://doi.org/10.1002/jbm.a.35495)

12. de Steiger RN, Pratt NL, Gulyani A, et al. Antibiotic utilisation in primary and revision total hip replacement patients: a registry linkage cohort study of 106 253 patients using the Australian Orthopaedic Association National Joint Replacement Registry. *Pharmacoepidemiol Drug Saf.* 2023;32(2):238-247. doi:[10.1002/pds.5522](https://doi.org/10.1002/pds.5522)
13. Elbuluk AM, Novikov D, Gotlin M, Schwarzkopf R, Iorio R, Vigdorchik J. Control strategies for infection prevention in total joint arthroplasty. *Orthop Clin North Am.* 2019;50(1):1-11. doi:[10.1016/j.ocl.2018.08.001](https://doi.org/10.1016/j.ocl.2018.08.001)
14. Eltohamy M, Kundu B, Moon J, Lee HY, Kim HW. Anti-bacterial zinc-doped calcium silicate cements: bone filler. *Ceram Int.* 2018;44(11):13031-13038. doi:[10.1016/j.ceramint.2018.04.122](https://doi.org/10.1016/j.ceramint.2018.04.122)
15. Peticone C, Thompson DDS, Dimov N, et al. Characterisation of osteogenic and vascular responses of hMSCs to Ti-Co doped phosphate glass microspheres using a microfluidic perfusion platform. *J Tissue Eng.* 2020;11. doi:[10.1177/2041731420954712](https://doi.org/10.1177/2041731420954712)
16. Jin HY, Xu L, Hou S. Preparation of spherical silica powder by oxygen-acetylene flame spheroidization process. *J Mater Process Technol.* 2010;210(1):81-84. doi:[10.1016/j.jmatprotec.2009.08.009](https://doi.org/10.1016/j.jmatprotec.2009.08.009)
17. De Silva Thompson D, Peticone C, Burova I, et al. Assessing behaviour of osteoblastic cells in dynamic culture conditions using titanium-doped phosphate glass microcarriers. *J Tissue Eng.* 2019;10. doi:[10.1177/2041731419825772](https://doi.org/10.1177/2041731419825772)
18. Gupta D, Hossain KMZ, Ahmed I, Sottile V, Grant DM. Flame-spheroidized phosphate-based glass particles with improved characteristics for applications in mesenchymal stem cell culture therapy and tissue engineering. *ACS Appl Mater Interfaces.* 2018;10(31):25972-25982. doi:[10.1021/acsami.8b05267](https://doi.org/10.1021/acsami.8b05267)
19. Lakhkar NJ, Park JH, Mordan NJ, et al. Titanium phosphate glass microspheres for bone tissue engineering. *Acta Biomater.* 2012;8(11):4181-4190. doi:[10.1016/j.actbio.2012.07.023](https://doi.org/10.1016/j.actbio.2012.07.023)
20. Eriksen EF. Cellular mechanisms of bone remodeling. *Rev Endocr Metab Disord.* 2010;11(4):219-227. doi:[10.1007/s11154-010-9153-1](https://doi.org/10.1007/s11154-010-9153-1)
21. Ge JF, Guo L, Wang S, et al. The size of mesenchymal stem cells is a significant cause of vascular obstructions and stroke. *Stem Cell Rev Rep.* 2014;10(2):295-303. doi:[10.1007/s12015-013-9492-x](https://doi.org/10.1007/s12015-013-9492-x)
22. Lakhkar NJ, Lee IH, Kim HW, Salih V, Wall IB, Knowles JC. Bone formation controlled by biologically relevant inorganic ions: role and controlled delivery from phosphate-based glasses. *Adv Drug Deliv Rev.* 2013;65(4):405-420. doi:[10.1016/j.addr.2012.05.015](https://doi.org/10.1016/j.addr.2012.05.015)
23. Hossain KMZ, Patel U, Kennedy AR, et al. Porous calcium phosphate glass microspheres for orthobiologic applications. *Acta Biomater.* 2018;72:396-406. doi:[10.1016/j.actbio.2018.03.040](https://doi.org/10.1016/j.actbio.2018.03.040)
24. Guedes JC, Park JH, Lakhkar NJ, Kim HW, Knowles JC, Wall IB. TiO<sub>2</sub>-doped phosphate glass microcarriers: a stable bioactive substrate for expansion of adherent mammalian cells. *J Biomater Appl.* 2013;28(1):3-11. doi:[10.1177/0885328212459093](https://doi.org/10.1177/0885328212459093)
25. Peticone C, De Silva Thompson D, Owens GJ, et al. Towards modular bone tissue engineering using Ti-Co-doped phosphate glass microspheres: cytocompatibility and dynamic culture studies. *J Biomater Appl.* 2017;32(3):295-310. doi:[10.1177/0885328217720812](https://doi.org/10.1177/0885328217720812)
26. Salih V, Patel A, Knowles JC. Zinc-containing phosphate-based glasses for tissue engineering. *Biomed Mater.* 2007;2(1):11-20. doi:[10.1088/1748-6041/2/1/003](https://doi.org/10.1088/1748-6041/2/1/003)
27. Li Q, Chang B, Dong H, Liu X. Functional microspheres for tissue regeneration. *Bioact Mater.* 2023;25:485-499. doi:[10.1016/j.bioactmat.2022.07.025](https://doi.org/10.1016/j.bioactmat.2022.07.025)

## SUPPORTING INFORMATION

Additional supporting information can be found online in the Supporting Information section at the end of this article.

**How to cite this article:** Tang T, Kang P, Verisqa F, Nguyen L, Knowles JC. Zinc phosphate glass microspheres promoted mineralization and expression of BMP2 in MC3T3-E1 cells. *J Biomed Mater Res.* 2024;112(12):2314-2328. doi:[10.1002/jbm.a.37781](https://doi.org/10.1002/jbm.a.37781)